Fitoterapia 146 (2020) 104672

Contents lists available at ScienceDirect

Fitoterapia

journal homepage: www.elsevier.com/locate/fitote

Rearranged neoclerodane diterpenoids from the aerial parts of *Salvia hispanica* L.

Min Fan[a,b], Dan Luo[a], Li-Yan Peng[a], Xing-De Wu[a], Xu Ji[a,c,*], Qin-Shi Zhao[a,*]

[a] State Key Laboratory of Phytochemistry and Plant Resources in West China, Kunming Institute of Botany, Chinese Academy of Sciences, Kunming 650204, PR China
[b] College of Pharmacy and Chemistry, Dali University, Dali 671000, PR China
[c] Key Laboratory of Medicinal Chemistry for Natural Resource, Ministry of Education and Yunnan Province, School of Chemical Science and Technology, Yunnan University, Kunming, Yunnan, PR China

ARTICLE INFO

Keywords:
Salvia hispanica L.
Neo-clerodane diterpenoids
Cardioprotective effects

ABSTRACT

Six new rearranged neoclerodane diterpenoids (**1**–**6**), as well as three known ones, were obtained from the aerial part of *Salvia hispanica* L. Their structures were elucidated by extensive analysis of spectroscopic data (1D, 2D NMR, and HRESIMS) and Mosher's method. The absolute configurations of **1**, **2**, and **4** were determined by single-crystal X-ray diffraction analysis. All isolated compounds were evaluated for their cardioprotective effects against H_2O_2-induced cardiomyocytes injury, and compound **5** showed statistically significant cardioprotective effect in vitro assays.

1. Introduction

The genus *Salvia* is the largest genus of plants in the Lamiaceae family, comprising over 1000 species distributed throughout the world. Many species in this genus have been used in folk medicine since ancient times due to its wide spectrum of activities [1]. *Salvia* genus is rich in diterpenes, including abietane, clerodane, pimarane and labdane diterpenoids [2]. Among them, clerodane diterpenes have attracted interest as a result of their noteworthy biological activities, involving insect antifeedant [3] and κ-opioid receptor agonistic activities [4].

Salvia hispanica L. is native to Mexico, and it is cultivated in Americas, Australia, and Southeast Asia for its seed oil [5]. The seeds of *S. hispanica* L., commonly known as chia seeds, were an important staple food for Mesoamericans in pre-Columbian times [6]. Our previous study on the title plant led to the isolation of twelve new neoclerodane diterpenoids, salvihispin A and its glycoside [7], and hispanins A-J [8]. In a continuation of our studies on the diterpenoid compounds from *Salvia* genus [9–12], we have now investigated the aerial part of *S. hispanica* L. From this plant we have isolated six new rearranged neoclerodane diterpenoids, representing clerodane diterpenoids with a rearranged clerodane scaffold with a 5/6/6/3/5 ring system for **1** [13], a salvigenane skeleton for **2** and **3**, a rearranged clerodane structure with an A/B spiro system for **4** and **5**, a rearranged clerodane structure with a 5/7/6/5 ring system for **6** (Fig. 1), along with three known compounds, 6,7-dihydrosalviandulin E (**7**) [14], 6,7-dehydrodugesin A (**8**) [15], and salviandolin E (**9**) [16].

In current study, the structures of all compounds were elucidated by various spectroscopic techniques, especially 2D NMR techniques and Mosher's method. Meanwhile, the absolute configurations of **1**, **2**, and **4** were also determined by single-crystal X-ray diffraction. Herein, the isolation, structural elucidation of these compounds, and their protective effects against H_2O_2-induced cardiomyocyte injury are reported.

2. Experimental

2.1. Gernal experimental procedures

The melting points were recorded with a WRX-4 micro-melting point apparatus. IR spectra were obtained by a Bruker Tensor-27 spectrometer with KBr pellets. Optical rotations were taken on a Horiba SEPA-300 polarimeter. UV spectra were obtained using a Shimadzu UV-2401A spectrophotometer. ESIMS and HRESIMS were performed on an Agilent 1290 UPLC/6540 Q-TOF. 1D (^{1}H, ^{13}C, and DEPT) and 2D (^{1}H–^{1}H COSY, HSQC, HMBC, and ROESY) spectra were recorded on a Bruker AV 600 spectrometer. MPLC was performed using a Lisui EZ Purify III System (Shanghai Lisui Chemical Engineering Company, Shanghai, China). An Agilent 1200 series instrument equipped with an Agilent Zorbax SB-C_{18} column (5 μm, 10 mm × 250 mm) was used for high-performance liquid chromatography (HPLC) analysis. Semipreparative HPLC were performed on an Agilent 1260

* Corresponding author at: State Key Laboratory of Phytochemistry and Plant Resources in West China, Kunming Institute of Botany, Chinese Academy of Sciences, Kunming 650204, PR China.
E-mail addresses: jixu@ynu.edu.cn (X. Ji), qinshizhao@mail.kib.ac.cn (Q.-S. Zhao).

https://doi.org/10.1016/j.fitote.2020.104672
Received 30 April 2020; Received in revised form 11 June 2020; Accepted 11 June 2020
Available online 15 June 2020
0367-326X/

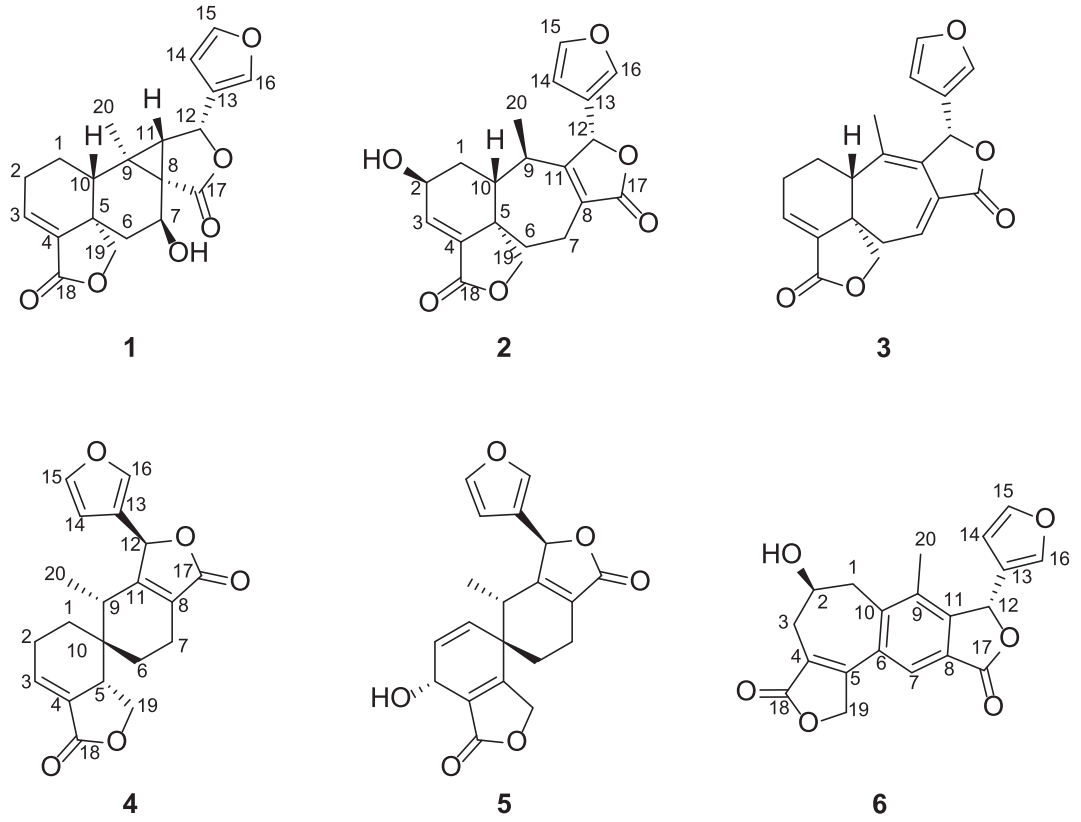

Fig. 1. Chemical structures of compounds **1–6**.

chromatography with a Zorbax SB-C_{18} column (9.4 mm × 25 cm). Column chromatography was performed using silica gel (100–200 and 200–300 mesh, Qingdao Marine Chemical Co. Ltd., Qingdao, China), MCI gel (CHP20P, 75–150 μm; Mitsubishi Chemical Corporation, Japan), and Sephadex LH-20 (Amersham Pharmacia Biotech, Sweden), and compounds were visualized by spraying the dried plates with 10% aqueous H_2SO_4 followed by heating until dryness. Petroleum ether, chloroform, ethyl acetate, acetone, 2-propanol, and methanol were purchased from Tianjing Chemical Reagents Co. (Tianjing, People's Republic of China).

2.2. Plant material

The aerial parts of *S. hispanica* L. were collected from Kunming Botanical Garden, Yunnan Province, which were cultivated and identified by Prof. Xiao Cheng of Kunming Institute of Botany, Chinese Academy of Sciences. A specimen of this plant was deposited at the State Key Laboratory of Phytochemistry and Plant Resources in West China, Kunming Institute of Botany, Chinese Academy of Sciences (voucher code 2015-10A-09B).

2.3. Extraction and isolation

The aerial parts of *S. hispanica* L. (26 kg) were shade dried, powdered, and extracted three times with acetone (100 L × 3, each 24 h) at room temperature. The resulting acetone extract was evaporated to dryness under reduced pressure, yielding crude extract (1.5 kg), which was subjected to a silica gel (100–200 mesh, 150 × 1500 mm, 7.0 kg) column chromatography and eluted with petroleum ether-acetone (100:0 to 0:100, v/v, 50 mL/min, each 10,000 mL) to give five fractions A-E. Of these, fraction C (300 g) was chromatographed by MPLC (MCI gel, 70 × 460 mm, 750 g), and eluted with EtOH-H_2O (50:50 to 100:0, v/v, 30 mL/min, each 4000 mL) to get eight fractions, C1-C8. Fraction C5 (37.1 g) was chromatographed by an RP-C_{18} column (70 × 460 mm, 100 g) and eluted with EtOH-H_2O (64:36 to 68:32, v/v, 30 mL/min, each 1000 mL) to afford three subfractions, C5a-C5c. Fraction C5b (10.3 g) was further purified by Sephadex LH-20 column (MeOH, 50 × 1500 mm, 500 g, 2000 mL), silica gel (200–300 mesh, 30 × 200 mm, 15 g) column (petroleum ether-EtOAc, 3:1, v/v, 500 mL), and semipreparative HPLC (MeOH-H_2O, 32:68, v/v, 5 mL/min) to afford **3** (10.5 mg, t_R 22.3 min), **9** (2.4 mg, t_R 26.5 min), and **4** (17.3 mg, t_R 35.7 min). Fraction E (270 g) was chromatographed by MPLC (MCI, 70 × 460 mm, 650 g) and eluted with EtOH-H_2O (40:60 to 100:0, v/v, 30 mL/min, each 4000 mL) to get eight fractions, E1-E8. Of these, fraction E5 (5.0 g) was subjected to a silica gel (200–300 mesh, 30 × 200 mm, 15 g) column chromatography and eluted with petroleum ether-$CHCl_3$-EtOAc (1:1:1, v/v/v, 500 mL) to give four subfractions, E5a-E5d. Fraction E5b (0.9 g) was further purified by a silica gel (200–300 mesh, 20 × 200 mm, 5 g) column chromatography (petroleum ether-$CHCl_3$–2-propanol, 8:100:4, v/v/v, 200 mL) and semipreparative HPLC (MeOH-H_2O, 23:77, v/v, 5 mL/min) to yield **6** (2.2 mg, t_R 32.3 min), **5** (4.2 mg, t_R 35.4 min), **2** (4.1 mg, t_R 43.4 min), and **8** (3.3 mg, t_R 54.2 min). Fraction E6 (25.2 g) was subjected to silica gel (200–300 mesh, 50 × 300 mm, 90 g) column chromatography and eluted with petroleum ether-$CHCl_3$-EtOAc (1:1:1, v/v/v, 1500 mL) to give five subfractions, E6a-E6e. Fraction E6e (2.5 g) was chromatographed on a silica gel (200–300 mesh, 20 × 200 mm, 10 g) column (petroleum ether-$CHCl_3$–2-propanol, 4:68:2, v/v/v, 200 mL), a Sephadex LH-20 column (MeOH, 20 × 1500 mm, 200 g), and a semipreparative HPLC (MeCN-H_2O, 28:72, v/v, 5 mL/min) to afford **1** (20.2 mg, t_R 30.2 min) and **7** (14.2 mg, t_R 45.7 min).

2.3.1. Salvihispin B (1)

Colorless, plate crystals (MeOH); mp 225–226 °C; $[\alpha]_D^{26}$ – 65.2 (*c* 0.09, MeOH); UV (MeOH) λ_{max} (log ε) 209 (4.12), 242 (3.17) nm; IR (KBr) ν_{max} 3426, 1762, 1631, 1384, 1247, 1208, 1022, 875, 743 and

Table 1
^{1}H NMR spectroscopic data for compounds **1–6** (δ in ppm, J in Hz).

No.	1[a]	2[a]	3[b]	4[b]	5[a]	6[c]
1a	1.88 (d, 12.6)	2.06 (m)	2.05 (m)	1.64 (m)	5.73 (d, 10.0)	3.19 (d, 14.3)
1b	1.40 (dd, 12.6, 3.8)	1.14 (td, 13.0, 4.1)	1.44 (ddd, 15.3, 12.1, 3.7)	1.44 (m)		3.07 (dd, 14.3, 8.2)
2a	2.45 (m)	4.44 (m)	2.54 (m)	2.46 (m)	6.05 (dd, 10.0, 3.6)	4.33 (m)
2b	2.23 (m)		2.08 (dt, 12.1, 2.2)	2.32 (m)		
3a	6.80 (dd, 7.5, 1.8)	6.88 (d, 6.6)	7.18 (dd, 8.0, 2.2)	6.89 (dd, 7.2, 4.0)	4.79 (d, 3.6)	2.83 (m)
3b						2.53 (m)
5				3.03 (m)		
6a	2.47 (m)	2.10 (dd, 14.0, 8.2)	2.84 (m)	1.97 (ddd, 13.9, 10.0, 6.7)	2.19 (ddd, 14.0, 10.7, 7.4)	
6b	1.02 (dd, 13.0, 8.9)	1.83 (m)	2.51 (m)	1.56 (dd, 13.9, 5.2)	2.06 (dd, 14.0, 6.7)	
7a	5.08 (t, 8.9)	2.81 (m)	7.07 (t, 3.8)	2.46 (m)	2.55 (dd, 10.7, 6.7)	7.79 (s)
7b		2.72 (ddd, 17.0, 8.2, 3.3)		2.32 (m)	2.46 (m)	
9		2.18 (m)		2.39 (q, 7.2)	2.63 (m)	
10	1.65 (dd, 12.6, 3.8)	2.85 (td, 13.0, 4.1)	2.85 (m)			
11	2.74 (d, 4.6)					
12	5.67 (d, 4.6)	6.08 (br s)	6.00 (s).	5.65 (s)	6.13 (s)	6.71 (s)
14	6.53 (s)	6.42 (s)	6.30 (s)	6.20 (br s)	6.39 (s)	6.24 (br s)
15	7.54 (br s)	7.57 (br s)	7.45 (overlapped)	7.43 (s)	7.56 (br s)	7.59 (t, 1.8)
16	7.59 (br s)	7.77 (s)	7.45 (overlapped)	7.54 (s)	7.76 (s)	7.85 (s)
19a	4.08 (s)	4.15 (d, 8.2)	3.90 (d, 8.5)	4.47 (t, 8.7)	4.96 (d, 17.9)	5.47 (d, 16.5)
19b		3.76 (dd, 8.2, 1.4)	3.57 (d, 8.5)	4.39 (t, 8.7)	4.86 (m)	5.26 (d, 16.5)
20	0.86 (s)	1.28 (d, 6.9)	1.83 (s)	0.78 (d, 7.2)	0.80 (d, 7.5)	2.28 (s)
OH						4.43 (d, 4.1)

[a] Recorded at 600 MHz in methanol-d_4;
[b] Recorded at 600 MHz in $CDCl_3$;
[c] Recorded at 600 MHz in acetone-d_6.

Table 2
^{13}C NMR spectroscopic data for compounds **1–6** (δ in ppm).

No.	1[a]	2[a]	3[b]	4[b]	5[a]	6[c]
1	23.9	34.6	25.9	31.1	135.9	36.3
2	27.4	63.0	24.6	23.7	129.6	70.1
3	138.2	134.8	139.0	135.9	59.3	39.2
4	136.6	140.5	134.7	127.7	129.5	125.3
5	46.7	46.2	45.3	45.4	165.8	154.4
6	41.3	36.2	43.0	28.7	33.9	127.0
7	63.7	19.4	138.2	17.7	19.3	121.4
8	32.9	125.3	126.3	125.8	127.5	133.9
9	41.1	37.3	136.0	34.0	38.1	134.0
10	50.0	37.0	46.7	37.5	44.1	145.9
11	39.4	167.8	130.5	164.8	164.9	149.8
12	74.9	77.7	73.5	77.6	77.6	75.7
13	123.2	121.6	123.2	120.9	121.4	122.6
14	110.2	108.9	108.3	108.1	109.4	109.6
15	145.0	145.9	144.6	144.5	145.8	145.4
16	141.1	143.2	140.5	141.3	143.9	143.8
17	177.3	175.8	169.6	172.3	174.3	169.9
18	171.6	172.2	169.3	169.3	174.3	174.6
19	71.2	73.1	70.9	68.3	73.0	71.0
20	13.1	18.4	16.4	15.9	12.2	15.9

[a] Recorded at 150 MHz in methanol-d_4;
[b] Recorded at 150 MHz in $CDCl_3$;
[c] Recorded at 150 MHz in acetone-d_6.

599 cm^{-1}; ^{1}H NMR and ^{13}C NMR data see Tables 1 and 2; ESIMS (positive) m/z 379 $[M + Na]^+$; HRESIMS (positive) m/z 379.1150 $[M + Na]^+$ (calcd for $C_{20}H_{20}O_6Na$, 379.1152).

2.3.2. Salvihispin C (2)

Colorless, prism crystals (MeOH); mp 286–287 °C; $[\alpha]_D^{26}$ – 113.4 (c 0.10, MeOH); UV (MeOH) λ_{max} (log ε) 210 (4.29) nm; IR (KBr) ν_{max} 3441, 2925, 1754, 1631, 1384, 1033, 875, 762 and 603 cm^{-1}; ^{1}H NMR and ^{13}C NMR data see Tables 1 and 2; ESIMS (positive) m/z 379 $[M + Na]^+$; HRESIMS (positive) m/z 379.1155 $[M + Na]^+$ (calcd for $C_{20}H_{20}O_6Na$, 379.1152).

2.3.3. Salvihispin D (3)

Colorless oil; $[\alpha]_D^{24}$ – 147.1 (c 0.08, MeOH); UV (MeOH) λ_{max} (log ε) 207 (3.93), 286 (3.28), 386 (2.97) nm; IR (KBr) ν_{max} 3432, 2925, 1761, 1636, 1201, 1021 and 602 cm^{-1}; ^{1}H NMR and ^{13}C NMR data see Tables 1 and 2; ESIMS (positive) m/z 377 $[M + K]^+$; HRESIMS (positive) m/z 377.0789 $[M + K]^+$ (calcd for $C_{20}H_{18}O_5K$, 377.0786).

2.3.4. Salvihispin E (4)

Yellow, prism crystals (MeOH); mp 242–243 °C; $[\alpha]_D^{24}$ – 87.7 (c 0.19, MeOH); UV (MeOH) λ_{max} (log ε) 212 (4.23) nm; IR (KBr) ν_{max} 3433, 2928, 1755, 1676, 1211, 1016, 874, 745 and 602 cm^{-1}; ^{1}H NMR and ^{13}C NMR data see Tables 1 and 2; ESIMS (positive) m/z 379 $[M + K]^+$; HRESIMS (positive) m/z 379.0944 $[M + K]^+$ (calcd for $C_{20}H_{20}O_5K$, 379.0942).

2.3.5. Salvihispin F (5)

Colorless oil; $[\alpha]_D^{26}$ – 29.7 (c 0.14, MeOH); UV (MeOH) λ_{max} (log ε) 208 (4.11), 274 (2.90) nm; IR (KBr) ν_{max} 3440, 2929, 1747, 1674, 1384, 1162, 1020, 875, 747 and 604 cm^{-1}; ^{1}H NMR and ^{13}C NMR data see Tables 1 and 2; ESIMS (positive) m/z 393 $[M + K]^+$; HRESIMS (positive) m/z 393.0735 $[M + K]^+$ (calcd for $C_{20}H_{18}O_6K$, 393.0735).

2.3.6. Salvihispin G (6)

Colorless oil; $[\alpha]_D^{26}$ – 158.4 (c 0.13, MeOH); UV (MeOH) λ_{max} (log ε) 196 (4.30), 241 (4.55), 274 (4.25) nm; IR (KBr) ν_{max} 3467, 1743, 1302, 1077, 1023, 980, 874, 757 and 602 cm^{-1}; ^{1}H NMR and ^{13}C NMR data see Tables 1 and 2; ESIMS (positive) m/z 375 $[M + Na]^+$; HRESIMS (positive) m/z 375.0840 $[M + Na]^+$ (calcd for $C_{20}H_{16}O_6Na$, 375.0839).

2.4. X-ray crystallographic analysis of 1, 2, and 4

The crystals of **1**, **2**, and **4** were used for measurement on a Bruker APEX DUO equipped with an APEX II CCD, using Cu Kα radiation. Cell refinement and data reduction were performed with Bruker SAINT. The structures of **1**, **2**, and **4** were solved by direct methods using SHELXS-2014. Refinements were performed with SHELXL-2014 using full-matrix least-squares. Non-hydrogen atoms were refined anisotropically. The H-atoms were placed in calculated positions and refined using a riding model. CCDC number 1864705, 1864706 and 1864707 respectively for compounds **1**, **2**, and **4**. These data can be obtained free of

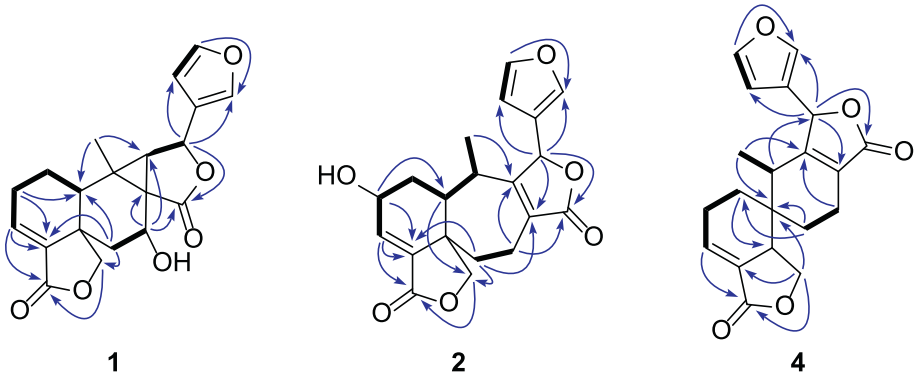

Fig. 2. $^{1}H-^{1}H$ COSY (thick lines) and selected HMBC (blue arrows) correlations of **1**, **2**, and **4**. (For interpretation of the references to colour in this figure legend, the reader is referred to the web version of this article.)

charge via http://www.ccdc.cam.ac.uk/conts/ retrieving.html (or from the CCDC, 12 Union Road, Cambridge CB21EZ, UK; fax: (+44)-1223-336-033; e-mail: deposit@ccdc.cam.ac.uk).

X-ray crystallography data of **1**: $C_{20}H_{20}O_6$, M = 356.36, a = 8.9333(4) Å, b = 9.4400(4) Å, c = 10.2381(5) Å, α = 90°, β = 100.596(2)°, γ = 90°, V = 848.66(7) Å^3, T = 100(2) K, space group $P21$, Z = 2, μ(CuKα) = 0.857 mm^{-1}, 5043 reflections measured, 2507 independent reflections (R_{int} = 0.0526). The final R_1 values were 0.1180 ($I > 2\sigma(I)$). The final $wR(F^2)$ values were 0.3018 ($I > 2\sigma(I)$). The final R_1 values were 0.1183 (all data). The final $wR(F^2)$ values were 0.3034 (all data). The goodness of fit on F^2 was 1.538. Flack parameter = 0.11(10).

X-ray crystallography data of **2**: $C_{20}H_{20}O_6$, M = 356.36, a = 9.2730(2) Å, b = 9.8624(2) Å, c = 18.7875(4) Å, α = 90°, β = 90°, γ = 90°, V = 1718.19(6) Å^3, T = 296(2) K, space group $P212121$, Z = 4, μ(CuKα) = 0.846 mm^{-1}, 10,712 reflections measured, 3132 independent reflections (R_{int} = 0.0274). The final R_1 values were 0.0399 ($I > 2\sigma(I)$). The final $wR(F^2)$ values were 0.1122 ($I > 2\sigma(I)$). The final R_1 values were 0.0403 (all data). The final $wR(F^2)$ values were 0.1129 (all data). The goodness of fit on F^2 was 1.066. Flack parameter = 0.00(6).

X-ray crystallography data of **4**: $C_{20}H_{20}O_5$, M = 340.36, a = 9.35780(10) Å, b = 11.7265(2) Å, c = 14.4453(2) Å, α = 90°, β = 90°, γ = 90°, V = 1585.14(4) Å^3, T = 100(2) K, space group $P212121$, Z = 4, μ(CuKα) = 0.841 mm^{-1}, 9305 reflections measured, 2810 independent reflections (R_{int} = 0.0267). The final R_1 values were 0.0277 ($I > 2\sigma(I)$). The final $wR(F^2)$ values were 0.0711 ($I > 2\sigma(I)$). The final R_1 values were 0.0277 (all data). The final $wR(F^2)$ values were 0.0711 (all data). The goodness of fit on F^2 was 1.072. Flack parameter = 0.07(4).

2.5. Protective effects against H_2O_2-induced cardiomyocytes injury assay

The protective effects on neonatal rat cardiomyocytes of compounds **1**–**9** (100 μM) were evaluated in a H_2O_2 injury model, and tanshinone IIA was used as the positive control [17]. Primary culture of neonatal rat cardiomyocytes were prepared from 1 to 3-day-old Wistar rats by trypsin as described previously [18]. The cells were pretreated with compounds for 24 h before exposure to H_2O_2 at the final concentration of 400 μM for 4 h. After the screening assays the effective compounds were selected for further study. The protective effects of effective compounds and tanshinone IIA at different concentrations (1, 10, and 100 μM) on neonatal rat cardiomyocytes injured by H_2O_2 were evaluated as described above.

3. Results and discussion

3.1. Chemistry

Salvihispin B (**1**) was isolated as colorless, plate crystals. The molecular formula of $C_{20}H_{20}O_6$ was determined by the HRESIMS ion at m/z 379.1150 $[M + Na]^+$ (calcd for $C_{20}H_{20}O_6Na$, 379.1152) with 11 degrees of unsaturation. The IR spectrum displayed the characteristic absorptions for hydroxy (3426 cm^{-1}) and carbonyl (1762 and 1631 cm^{-1}) functionalities. The ^{1}H NMR data of **1** (Table 1) showed the presence of one methyl group (δ_H 0.86, s, H_3–20), one olefinic proton (δ_H 6.80, dd, J = 7.5, 1.8 Hz, H-3), and a typical β-substituted furan ring [δ_H 6.53 (s, H-14); 7.54 (br s, H-15); 7.59 (br s, H-16)]. The ^{13}C and DEPT NMR spectra exhibited 20 carbon signals including one methyl, four methylenes (one oxygenated), eight methines (two oxygenated and four olefinic), seven quaternary carbons (two ester carbonyls and two olefinic). As six of 11 degrees of unsaturation were accounted for two ester carbonyls, a double bond, and a furan ring, the remain degrees of unsaturation required additional five rings in the structure. The above spectroscopic analysis suggested that compound **1** was a neoclerodane diterpenoid [13]. The ^{1}H and ^{13}C NMR data of **1** (Tables 1 and 2) were almost identical to those of salvileucanthsin A [14], which was obtained previously from *S. leucantha*. The major difference between their NMR spectra was the presence of a methylene (δ_H/δ_C 2.45, 2.23/27.4) and the absence of a oxygenated methine in **1**, suggesting that **1** was a deoxygenated derivative of salvileucanthsin A. The methylene group at C-2 was confirmed by HMBC correlations (Fig. 2) of H_2–2 [δ_H 2.45 (m), 2.23 (m)] with C-4 (δ_C 136.6) and C-10 (δ_C 50.0), together with the $^1H-^1H$ COSY correlations of H-10/H_2–1/H_2–2/H-3. The ROSEY correlations (Fig. 3) of H-7/H_2–19 and H_2–19/H_3–20 suggested that they were co-facial and adopted α-orientations, whereas the ROESY correlations of H-16/H_3–20 suggested the β-orientation of H-12. H-10 and H-11 were assigned to be β-oriented based on the ROESY correlations of H-6a/H-19a, H-6b/H-10, and H-10/H-11. Finally, a single-crystal X-ray diffraction analysis (Fig. 4) was performed to establish the absolute configuration of **1** as 5*S*,7*S*,8*S*,9*S*,10*R*,11*S*,12*R*.

Salvihispin C (**2**) was isolated as colorless prism crystals with a molecular formula of $C_{20}H_{20}O_6$, as shown by its HRESIMS data $[M + Na]^+$ m/z 379.1155 (calcd 379.1152). The IR absorptions showed the presence of hydroxy (3441 cm^{-1}) and carbonyl (1754 and 1631 cm^{-1}) functionalities. The ^{1}H NMR data (Table 1) indicated the presence of a β-substituted furan ring [δ_H 6.42 (s, H-14); 7.57 (br s, H-15); 7.77 (s, H-16)] and a methyl group at δ_H 1.28 (d, J = 6.9 Hz, H-20). The ^{13}C NMR and DEPT data (Table 2) exhibited 20 carbons attributed to one methyl, four methylenes (one oxygenated), eight methines (two oxygenated and four olefinic), and seven quaternary carbons (two ester carbonyls and four olefinic). The ^{1}H and ^{13}C NMR data of **2** (Tables 1 and 2) were similar to those of dugesin D [19]. The only

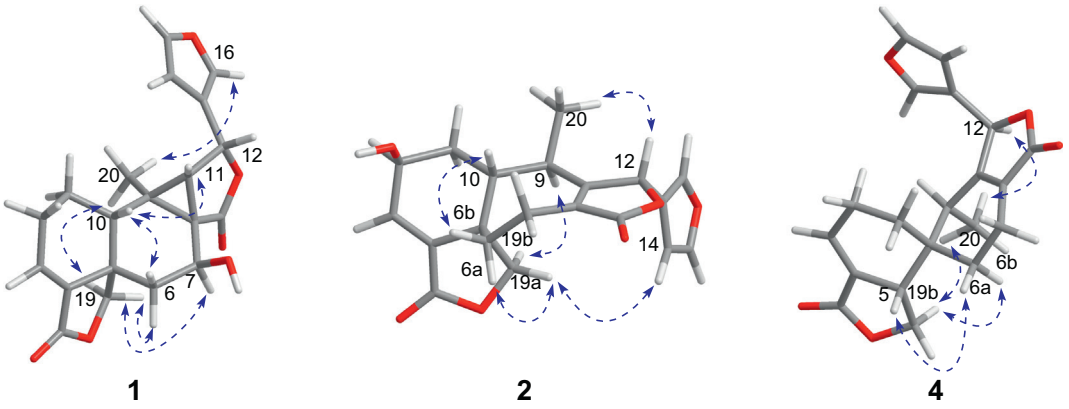

Fig. 3. ROESY correlations of compounds **1**, **2**, and **4**.

distinction between these two compounds was the location of the hydroxy group at C-2 in **2** rather than at C-6 in the latter, which were confirmed by the HMBC correlations (Fig. 2) of H-2 [δ_H 4.44 (m)] with C-4 (δ_C 140.5), C-10 (δ_C 37.0), and of H_2–6 [(δ_H 2.10 (dd, J = 14.0, 8.2 Hz), 1.83 (m)] with C-4, C-8 (δ_C 125.3), C-19 (δ_C 73.1), as well as the $^1H-^1H$ COSY correlations (Fig. 2) of H_3–20/H-9/H-10/H_2–1/H-2/H-3. The ROESY correlations (Fig. 3) of H-6a/H-19a, H-14/H-19a, H-6b/H-10, and H-12/H_3–20 indicated H-10, H-12, and H_3–20 were β-oriented. The small coupling constant of $J_{1b/2}$ (2.1 Hz) was indicative of a β-orientation for 2-OH group. Finally, compound **2** was crystallized from MeOH to obtain colorless prism crystals, which was then subjected to X-ray diffraction analysis (Fig. 4) with Cu Kα radiation. The absolute configuration of **2** was finally determined as 2*S*,5*S*,9*R*,10*R*,12*R* by Flack parameter 0.00(6).

Salvihispin D (**3**) was assigned as the molecular formula of $C_{20}H_{18}O_5$ based on HRESIMS ion at m/z 377.0789 $[M + K]^+$ (calcd for $C_{20}H_{18}O_5K$, 377.0786) and ^{13}C NMR spectroscopic data. Its ^1H and ^{13}C NMR data (Tables 1 and 2) were comparable to those of dugesin A [20], except that the double bonds migrated from C-8/C-11 and C-9/C-10 in dugesin A to C-7/C-8 and C-9/C-11 in **3**, respectively. These assumptions were supported by the HMBC correlations of H-7 [δ_H 7.07 (t, J = 3.8 Hz)] with C-5 (δ_C 45.3), C-8 (δ_C 126.3), C-11 (δ_C 130.5) and C-17 (δ_C 169.6), of H-10 [δ_H 2.85 (m)] and H-12 [δ_H 6.00 (s)] with C-9 (δ_C 136.0) and C-11. The ROESY correlations of H-10/H-6b, H-19a/H-6a, H-19a/H-14 indicated that H-10 and H-12 were β-oriented. Therefore, the relative configuration of **3** was identical to those of dugesin A, and **3** was named salvihispin D.

Salvihispin E (**4**) was isolated as a yellow, prism crystals, and its molecular formula was established as $C_{20}H_{20}O_5$ on the basis of its ^{13}C NMR data and molecular ion peak at m/z 379.0944 $[M + K]^+$ (calcd for $C_{20}H_{20}O_5K$, 379.0942) in the positive-ion HRESIMS. The ^1H and ^{13}C NMR data (Tables 1 and 2) of **4** were quite similar to those of dugesin C [19], with the exception that a methyl (δ_H/δ_C 0.78/15.9) of C-20 and a methine (δ_H/δ_C 2.39/34.0) of C-9 in **4** replaced the exocyclic double bond in the latter. This observation suggested that **4** was the 9,20-dihydro derivative of dugesin C, which was confirmed by the proton spin system (H-9/H_3–20) observed from the $^1H-^1H$ COSY spectrum (Fig. 2) and the HMBC correlations (Fig. 2) from H_3–20 [δ_H 0.78 (d, J = 7.2 Hz)] to C-10 (δ_C 37.5), and C-11 (δ_C 164.8). The ROESY correlations (Fig. 3) of H-12/H_3–20, H_2–19/H_3–20 suggested α-orientations of H-12, H_2–19, and H_3–20, and the *S** configuration for C-10. The correlations of H-5/H-6a, H-19b/H-6b indicated the β-orientation of H-5. Finally, the absolute configuration of **4** was determined as 5*S*,9*S*,10*S*,12*S* by single-crystal X-ray diffraction (Fig. 4). Thus, the structure of **4** was established as depicted.

Salvihispin F (**5**) was obtained as colorless oil. Its HRESIMS showed a peak at m/z 393.0735 $[M + K]^+$ (calcd for $C_{20}H_{18}O_6K$, 393.0735), which in conjunction with the ^{13}C NMR data, corresponding to a molecular formula of $C_{20}H_{18}O_6$. The IR spectrum showed absorptions for hydroxy and carbonyl groups at 3440 and 1747 cm^{-1}, respectively. The ^1H and ^{13}C NMR spectra of **5** (Tables 1 and 2) closely resembled those of **4**. A major difference was presence of Δ^1 and Δ^4 double bonds in **5**

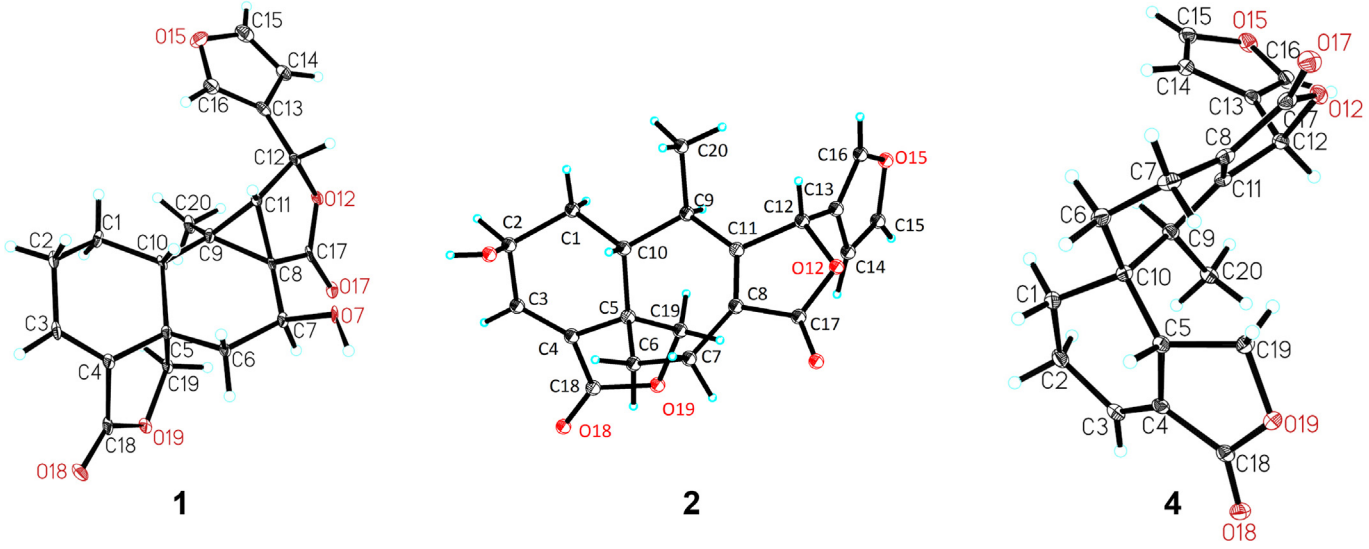

Fig. 4. X-ray crystallography structures of compounds **1**, **2** and **4**.

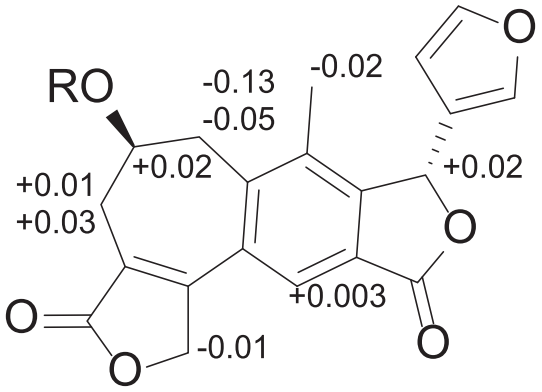

6*R*: R = (*R*)-MTPA

6*S*: R = (*S*)-MTPA

Fig. 5. Results with Mosher's method ($\Delta\delta_H = \delta_S - \delta_R$).

rather than Δ^3 double bond in **4**, which were corroborated by the HMBC correlations of H_2–6 [2.19 (ddd, J = 14.0, 10.7, 7.4 Hz), 2.06 (dd, J = 14.0, 6.7 Hz)] and H-9 (2.63, m) with C-1 (δ_C 135.9) and C-5 (δ_C 165.8), and of H-3 and H_2–19 [4.96 (d, J = 17.9 Hz), 4.86 (m)] with C-4 (δ_C 129.5) and C-5, as well as the $^1H-^1H$ COSY correlations of H-1/H-2/H-3. The other difference was the existence of a hydroxy group at C-3 in **5**, which was confirmed by the HMBC correlations of H-3 [δ_H 4.79 (d, J = 3.6 Hz)] with C-2 (δ_C 129.6), C-4, and C-5. Clear ROESY correlations of H-12/H_3–20, H-19b/H_3–20, H-9/H-6a and H-3/H-6b indicated the α-orientations of H-12 and H_3–20, β-orientation of H-3, and the R^* configuration for C-10. The structure of **5** was thus confirmed as shown.

Salvihispin G (**6**) was obtained as colorless oil. Its HRESIMS spectra exhibited a peak at m/z 375.0840 $[M + Na]^+$ (calcd for $C_{20}H_{16}O_6Na$, 375.0839) and yielded a molecular formula of $C_{20}H_{16}O_6$, suggesting 13 degrees of unsaturation. The absorption bands at 3467 and 1743 cm^{-1} in the IR spectrum indicated the presence of hydroxy and carbonyl functionalities, respectively. The ^{13}C NMR and DEPT spectra (Table 2) showed 20 carbon signals including one methyl, three methylenes (one oxygenated), six methines (two oxygenated and four olefinic), and ten quaternary carbons (two ester carbonyls and eight olefinic). Analyzing its NMR data (Tables 1 and 2) revealed that its structure resembled that of salvileucanthsin C [14], except for the absence of a hydroxy group at C-1 in **6**, indicating that **6** was deoxygenated derivative of salvileucanthsin C, which were supported by the $^1H-^1H$ COSY correlations of H_2–1/H-2/H_2–3. The modified Mosher's method [21] was applied to determine the absolute configuration of the secondary alcohol at C-2 in **6**. As shown in Fig. 5, the values of $\Delta\delta_H$ ($\Delta\delta_H = \delta_S - \delta_R$) for H_2–3 were positive, while a negative $\Delta\delta_H$ value was observed for H_2–1. Thus, the absolute configuration at C-2 was assigned as *S*. Since the optical rotation of **6** were identical to that of salvileucanthsin C [14], and taking the same biogenetic into consideration, the absolute configuration of C-12 should be *R* as same as salvileucanthsin C. Thus, according to the above evidence, the absolute configuration of **6** was assigned as 2*S*,12*R*.

A plausible biosynthetic pathway for **1–9** is proposed as shown in Scheme 1. Compound **3** might produce intermediates **a** and **g** via isomerization. Intermediate **a** was transformed to compound **1** through oxidation, Wagner-Meerwein rearrangement, and reduction. Reduction, oxidation, dehydration and aromatization may lead to the formation of compounds **2** and **6** from intermediate **a**. Intermediate **g** was transformed to compounds **7** and **9** through oxidation and aromatization, respectively. Oxidation, dehydration and reduction of intermediate **g** might lead to the formation of compounds **4** and **5**. Finally, compound **9** was transformed to **8** through oxidation.

3.2. Biological activity

The isolated compounds **1–9** were evaluated for their cardioprotective effects against H_2O_2-induced cardiomyocytes injury by MTS assay. Tanshinone IIA was used as the positive control, which had protective effects against cardiomyocytes injury [17]. The viabilities of cardiomyocytes pre-treated with compounds **1–9** at 100 μM on neonatal rat cardiomyocytes from H_2O_2 injury were first evaluated, and the

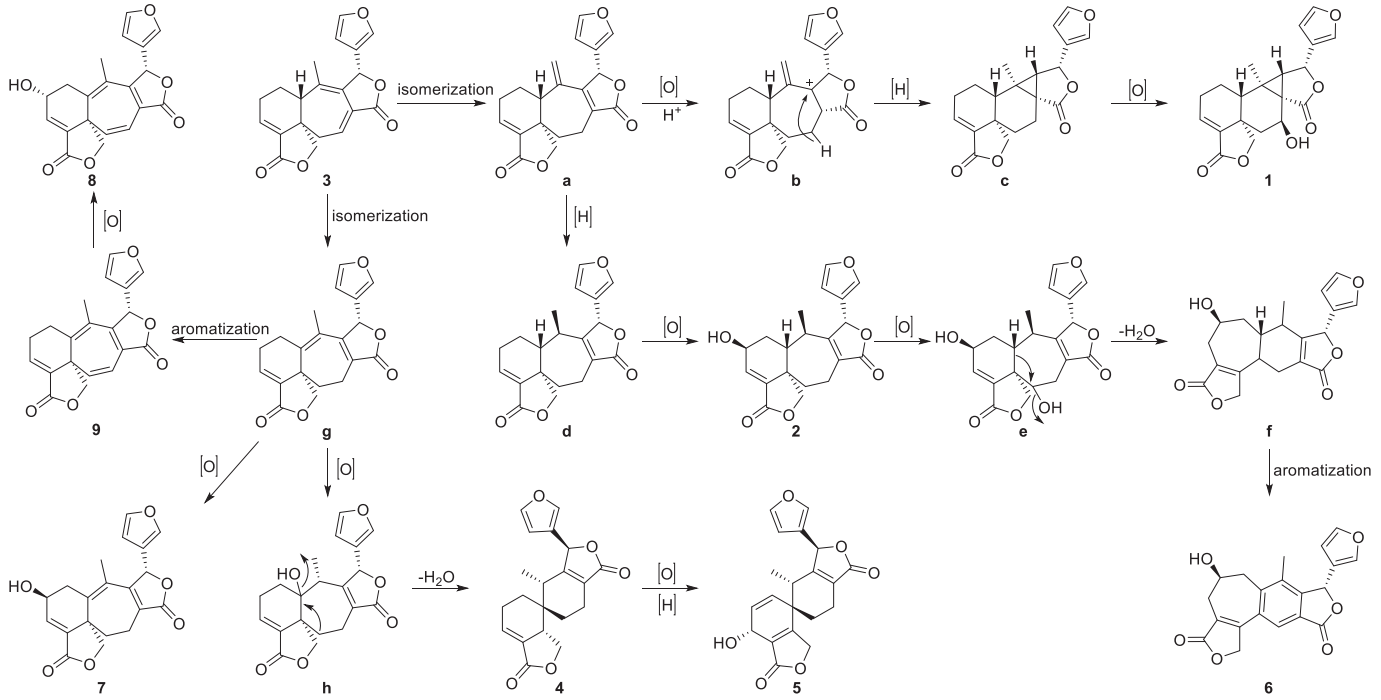

Scheme 1. Putative biosynthetic pathways for compounds **1–9**.

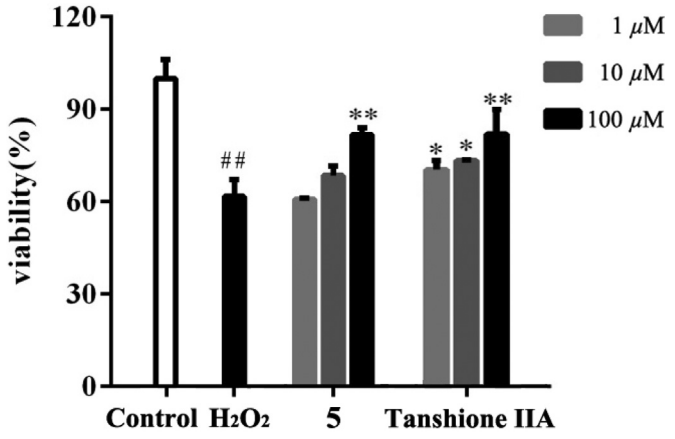

Fig. 6. Protective effects of compound **5** against H_2O_2-induced cardiomyocytes injury at different concentrations. Data expressed as means ± SD ($n = 3$). $^{*}P < 0.05$, $^{**}P < 0.01$ vs vehicle group (0 μM).

results showed that only compound **5** showed potent activity, which was comparable to that of the positive control. Moreover, compound **5** demonstrated a dose-dependent manner with the concentration from 1 to 100 μM, increased the cell viability to 60.8 ± 0.3%, 68.5 ± 3.1% and 81.9 ± 2.2% at concentrations of 1, 10 and 100 μM, respectively (Fig. 6).

Declaration of Competing Interest

The authors declare that there is no conflict of interest.

Acknowledgments

This work was supported by the project of the Natural Science Foundation of China (Nos. 21837003 and 81773611), the Joint Foundation of NSFC-Yunnan Province (No. U1502223), the Science and Technology Program of Yunnan Province (No. 2018ZF001), and the CAS "Light of West China" Program and Youth Innovation Promotion Association CAS (X.-D. Wu).

Appendix A. Supplementary data

The 1D NMR, 2D NMR, IR, and HRESIMS spectra for compounds **1–6**, are available in the Supplementary data for this article can be found online at https://doi.org/10.1016/j.fitote.2020.104672

References

[1] G.P.P. Kamatou, N.P. Makunga, W.P.N. Ramogola, A.M. Viljoen, South African *Salvia* species: a review of biological activities and phytochemistry, J. Ethnopharmacol. 119 (2008) 664–672.
[2] Y.B. Wu, Z.Y. Ni, Q.W. Shi, M. Dong, H. Kiyota, Y.C. Gu, B. Cong, Constituents from *Salvia* species and their biological activities, Chem. Rev. 112 (2012) 5967–6026.
[3] R.D. Enriz, H.A. Baldoni, M.A. Zamora, E.A. Jauregui, M.E. Sosa, C.E. Tonn, J.M. Luco, M. Gordaliza, Structure-antifeedant activity relationship of clerodane diterpenoids. Comparative study with withanolides and azadirachtin, J. Agric. Food Chem. 48 (2000) 1384–1392.
[4] B.L. Roth, K. Baner, R. Westkaemper, D. Siebert, K.C. Rice, S. Steinberg, P. Ernsberger, R.B. Rothman, Salvinorin A: a potent naturally occurring non-nitrogenous κ opioid selective agonist, Proc. Natl. Acad. Sci. U. S. A. 99 (2002) 11934–11939.
[5] W. Jamboonsri, T.D. Phillips, R.L. Geneve, J.P. Cahill, D.F. Hildebrand, Extending the range of an ancient crop, *Salvia hispanica* L.—a new ω3 source, Genet. Resour. Crop Ev. 59 (2012) 171–178.
[6] E. Reyes-Caudillo, A. Tecante, M.A. Valdivia-Lopez, Dietary fibre content and antioxidant activity of phenolic compounds present in Mexican chia (*Salvia hispanica* L.) seeds, Food Chem. 107 (2008) 656–663.
[7] M. Fan, Y. Zhu, Z.J. Zhang, R.N. Du, Q.F. Zhu, X.D. Wu, Q.S. Zhao, Salvihispin A and its glycoside, two *neo*-clerodane diterpenoids with neurotrophic activities from *Salvia hispanica* L, Tetrahedron Lett. 59 (2018) 143–146.
[8] M. Fan, D. Luo, L.Y. Peng, X.N. Li, X.D. Wu, X. Ji, Q.S. Zhao, Neo-clerodane diterpenoids from aerial parts of *Salvia hispanica* L. and their cardioprotective effects, Phytochemistry 166 (2019) 112065.
[9] G. Xu, A.J. Hou, Y.T. Zheng, Y. Zhao, X.L. Li, L.Y. Peng, Q.S. Zhao, Przewalskin B, a novel diterpenoid with an unprecedented skeleton from *Salvia przewalskii* Maxim, Org. Lett. 9 (2007) 291–293.
[10] G. Xu, A.J. Hou, R.R. Wang, G.Y. Liang, Y.T. Zheng, Z.Y. Liu, X.L. Li, Y. Zhao, S.X. Huang, L.Y. Peng, Q.S. Zhao, Przewalskin A: a new C23 terpenoid with a 6/6/7 carbon ring skeleton from *Salvia przewalskii* Maxim, Org. Lett. 8 (2006) 4453–4456.
[11] L.W. Li, Y.Y. Qi, S.X. Liu, X.D. Wu, Q.S. Zhao, *Neo*-clerodane and abietane diterpenoids with neurotrophic activities from the aerial parts of *Salvia leucantha* Cav, Fitoterapia 127 (2018) 367–374.
[12] Y.J. Jiang, Y. Zhang, J. He, X.D. Wu, L.D. Shao, X.N. Li, J. Su, L.Y. Peng, R.T. Li, Q.S. Zhao, (±)-Salviaprione, a pair of unprecedented abietane-type diterpenoids from *Salvia prionitis*, Tetrahedron Lett. 56 (2015) 5457–5459.
[13] R.T. Li, S.L. Morris-Natschke, K.-H. Lee, Clerodane diterpenes: sources, structures, and biological activities, Nat. Prod. Rep. 33 (2016) 1166–1226.
[14] Y.J. Jiang, J. Su, X. Shi, X.D. Wu, X.Q. Chen, J. He, L.D. Shao, X.N. Li, L.Y. Peng, R.T. Li, Q.S. Zhao, *neo*-Clerodanes from the aerial parts of *Salvia leucantha*, Tetrahedron 72 (2016) 5507–5514.
[15] Y. Aoyagi, K. Fujiwara, A. Yamazaki, N. Sugawara, R. Yano, H. Fukaya, Y. Hitotsuyanagi, K. Takeya, A. Ishiyama, M. Iwatsuki, K. Otoguro, H. Yamada, S. Omura, Semisynthesis of salviandulin E analogues and their antitrypanosomal activity, Bioorg. Med. Chem. Lett. 24 (2014) 442–446.
[16] B. Esquivel, R.M. Dominguez, S. Hernández-Ortega, R.A. Toscano, L. Rodríguez-Hahn, Salvigenane and isosalvipuberulan diterpenoids from *Salvia leucantha*, Tetrahedron 50 (1994) 11593–11600.
[17] J.J. Fu, H.Q. Huang, J.J. Liu, R.B. Pi, J.W. Chen, P.Q. Liu, Tanshinone IIA protects cardiac myocytes against oxidative stress-triggered damage and apoptosis, Eur. J. Pharmacol. 568 (2007) 213–221.
[18] Y.J. Lu, Y. Zhang, H.L. Shan, Z.W. Pan, X.L. Li, B.X. Li, C.Q. Xu, B.S. Zhang, F.M. Zhang, D.L. Dong, MicroRNA-1 downregulation by propranolol in a rat model of myocardial infarction: a new mechanism for ischaemic cardioprotection, Cardiovasc. Res. 84 (2009) 434–441.
[19] X. Gang, Z. Fang, X.W. Yang, J. Zhou, L.X. Yang, X.L. Shen, Y.J. Hu, Q.S. Zhao, *neo*-Clerodane diterpenoids from *Salvia dugesii* and their bioactive studies, Nat. Prod. Bioprospect. 1 (2011) 81–86.
[20] G. Xu, L.Y. Peng, X.M. Niu, Q.S. Zhao, R.T. Li, H.D. Sun, Novel diterpenoids from *Salvia dugesii*, Helv. Chim. Acta 87 (2004) 949–955.
[21] I. Ohtani, T. Kusumi, Y. Kashman, H. Kakisawa, High-field FT NMR application of Mosher's method. The absolute configurations of marine terpenoids, J. Am. Chem. Soc. 113 (1991) 4092–4096.